Physiological characterization of human muscle acetylcholine receptors from ALS patients

Eleonora Palma[a,b,1,2], Maurizio Inghilleri[c,1], Luca Conti[a], Cristina Deflorio[a], Vittorio Frasca[c], Alessia Manteca[a], Floriana Pichiorri[c], Cristina Roseti[a,b], Gregorio Torchia[a], Cristina Limatola[a], Francesca Grassi[a], and Ricardo Miledi[d,e,2]

[a]Istituto Pasteur-Fondazione Cenci Bolognetti, Dipartimento di Fisiologia e Farmacologia, Università Sapienza, 00185 Rome, Italy; [b]Istituto di Ricovero e Cura a Carattere Scientifico San Raffaele Pisana, 00166 Rome, Italy; [c]Dipartimento di Neurologia e Psichiatria, Università Sapienza, 00185 Rome, Italy; [d]Instituto de Neurobiología, Universidad Nacional Autónoma de México, AP1-1141, Querétaro, México; and [e]Department of Neurobiology and Behavior, University of California, Irvine, CA 92697-4550

Contributed by Ricardo Miledi, November 3, 2011 (sent for review October 13, 2011)

Amyotrophic lateral sclerosis (ALS) is characterized by progressive degeneration of motor neurons leading to muscle paralysis. Research in transgenic mice suggests that the muscle actively contributes to the disease onset, but such studies are difficult to pursue in humans and in vitro models would represent a good starting point. In this work we show that tiny amounts of muscle from ALS or from control denervated muscle, obtained by needle biopsy, are amenable to functional characterization by two different technical approaches: "microtransplantation" of muscle membranes into *Xenopus* oocytes and culture of myogenic satellite cells. Acetylcholine (ACh)-evoked currents and unitary events were characterized in oocytes and multinucleated myotubes. We found that ALS acetylcholine receptors (AChRs) retain their native physiological characteristics, being activated by ACh and nicotine and blocked by α-bungarotoxin (α-BuTX), d-tubocurarine (dTC), and galantamine. The reversal potential of ACh-evoked currents and the unitary channel behavior were also typical of normal muscle AChRs. Interestingly, in oocytes injected with muscle membranes derived from ALS patients, the AChRs showed a significant decrease in ACh affinity, compared with denervated controls. Finally, riluzole, the only drug currently used against ALS, reduced, in a dose-dependent manner, the ACh-evoked currents, indicating that its action remains to be fully characterized. The two methods described here will be important tools for elucidating the role of muscle in ALS pathogenesis and for developing drugs to counter the effects of this disease.

voltage-clamp | patch-clamp

Amyotrophic lateral sclerosis (ALS) is a rare but fatal disease caused by a progressive degeneration of motor neurons that occurs sporadically in over 90% of the patients. Except for a minority of genetic causes, the etiology of the disease is still unknown, but there is a general consensus that multiple mechanisms combine to cause the pathology (1). To date, no effective treatment exists, although the lifespan of ALS patients can be slightly increased by riluzole, the only drug approved for treatment of ALS (2).

The hallmark of the pathology is the selective death of upper and/or lower motor neurons, but several researchers point out that muscle denervation precedes neuronal death in mouse models of the pathology, according to the so-called "dying back" model of neuronal death (3, 4). It has been proposed that muscle actively contributes to motor neuron degeneration, possibly by releasing factors that inhibit neurite outgrowth (5, 6). Endplate acetylcholine receptors (AChRs) might also play a role in the disease, as their silencing mimics axotomy by increasing the excitability of motor neurons in wild-type mice (7). However, these hypotheses are largely based on data obtained in transgenic mice expressing various mutant forms of the human SOD1 enzyme, which in humans accounts for a minority of cases; only one case of human disease has been evaluated in this regard (8). Whether taking place early or late in disease, muscle denervation is an inescapable feature of ALS and, among other effects, it has a deep impact on AChR composition and distribution. In normally innervated muscle fibers, AChRs are composed of α_1-, β_1-, ε-, and δ-subunits (ε-AChR) and are clustered at high density at the nerve–muscle and muscle–tendon junctions (9–11).

Upon denervation, ACh supersensitivity occurs: extrasynaptic nuclei resume transcription of AChR subunit genes, and receptors containing α_1, β_1, γ, and δ (γ-AChRs) appear over the entire sarcolemma (12–14). The AChR isoforms differ in conductance and kinetics, as well as in ion selectivity, both in rodents and humans (15, 16). Riluzole produces a slight reduction in the ACh-evoked currents in cells expressing recombinant mouse ε-AChRs (17), although only if used at high, nonclinical concentrations (2), raising concerns about possible side effects on neuromuscular transmission. All these open questions make it clear that new experimental systems allowing a detailed investigation of muscle abnormalities in human cases of ALS may provide insight into the pathogenesis and treatment of the disease.

In this work we took advantage of the oocyte microtransplantation technique (18, 19) to study the function of muscle AChRs of ALS patients. This approach allows the exploitation of tiny muscle fragments obtained by needle biopsies, thus minimizing the patient's discomfort. In parallel experiments, some muscle fragments were cultured to derive satellite cells and hence polynucleated myotubes, from which ACh-evoked whole-cell and unitary currents were recorded despite the limited differentiative capability of satellite cells from ALS patients (20). In these two preparations we tested the effects of riluzole and other drugs considered potentially useful therapeutic tools for ALS. The results obtained indicate that both experimental systems have the potential to become highly valuable for investigation of the role of muscle in the onset and progression of sporadic ALS, as well as to test the direct and possibly unwanted side effects of any drug proposed as a therapeutic agent for ALS.

Results

Functional Expression of Native AChRs from Human Muscles in *Xenopus* Oocytes. Injections of *Xenopus* oocytes with membranes extracted from muscle specimens of 13 of the 19 ALS patients (P) studied (P1–12 and P17 in Table S1) and 8 of 9 denervated control patients (P20–22 and P24–28) (Table S1) led to the incorporation of functional AChRs into the oocyte membrane. Application of

Author contributions: E.P., M.I., F.G., and R.M. designed research; E.P., M.I., L.C., C.D., V.F., A.M., F.P., C.R., G.T., F.G., and R.M. performed research; C.L. contributed new reagents/analytic tools; E.P., M.I., L.C., C.D., V.F., A.M., F.P., C.R., G.T., F.G., and R.M. analyzed data; and E.P., M.I., F.P., C.L., F.G., and R.M. wrote the paper.

The authors declare no conflict of interest.

[1]E.P. and M.I. contributed equally to this work.

[2]To whom correspondence may be addressed. E-mail: eleonora.palma@uniroma1.it or rmiledi@uci.edu.

This article contains supporting information online at www.pnas.org/lookup/suppl/doi:10.1073/pnas.1117975108/-/DCSupplemental.

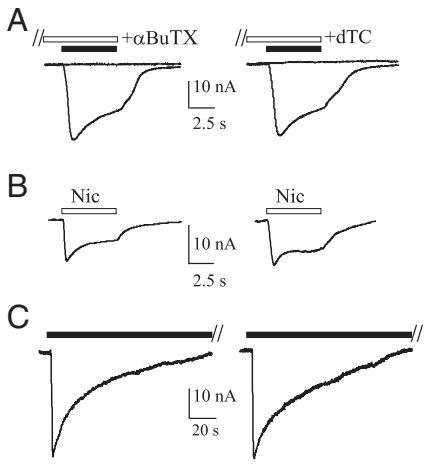

Fig. 1. Nicotinic AChRs are incorporated by oocytes injected with muscle membranes from ALS or denervated patients. (*A*, *Left*). Superimposed currents elicited by 100 μM ACh before and after pretreatment with 5 μM αBuTX in 1 oocyte, representative of 10, microinjected with muscle membranes from one ALS patient (P1). (*Right*) Sample traces elicited by 100 μM ACh before and after 10 μM dTC in 1 oocyte, representative of 15, injected with muscle membranes from the same patient. In this and subsequent figures, horizontal filled bars indicate the timing of ACh applications and open bars that of drug applications. Holding potential was −60 mV. Note the complete block of ACh-evoked currents after αBuTX or dTC. (*B*) Typical currents evoked by nicotine (500 μM, open bars) in 2 oocytes, representative of 10, injected with muscle membranes from one ALS (P1; *Left*) and one denervated patient (P20; *Right*). (*C*) The current decay during prolonged ACh applications (250 μM for 2 min) is similar in oocytes injected with muscle membranes from one ALS (P5; *Left*) and one denervated patient (P21; *Right*). Experiments are representative of 15 oocytes.

ACh to these cells (5 μM to 1 mM; Figs. 1 and 2) elicited an inward current, the peak amplitude of which depended on transmitter concentration, whereas noninjected oocytes showed no detectable responses to ACh. Muscle membranes microtransplanted from a few patients (P13, 16, 18, 19, and 23) did not elicit detectable responses to ACh, probably due to the small number of functional AChRs incorporated into the oocyte plasma membrane.

In oocytes injected with muscle membranes from ALS patients, ACh (100 μM at −60 mV) elicited a current (I_{ACh}) with mean peak amplitude of −16.4 ± 2.4 nA [mean ± SEM; 123 oocytes/28 frogs (123/28); range, −5 to −31 nA, Fig. 1*A*]. Currents of similar amplitude were recorded from oocytes injected with muscle membranes from denervated control patients (−14.2 ± 5 nA; 66/2; range, −4 to −30 nA, Fig. 1*A*). Those currents were caused by activation of transplanted functional AChRs because they were blocked by the classical antagonists of nicotinic AChRs, α-bungarotoxin (αBuTX) (5 μM, 30 min of pretreatment; 10/2; P1, P5, P20, and P21, Fig.1*A*) and d-tubocurarine (dTC) (10 μM, 2 min of pretreatment; 15/3; P1, P5, and P20; Fig. 1*A*). Moreover, the currents were activated by nicotine (0.5 or 1 mM, Fig. 1*B*), consistent with the effects of antagonists on activation of nicotinic AChRs derived from the injected membranes.

Functional Characteristics of AChRs from Human Muscles. Experiments were aimed at comparing the functional characteristics of I_{ACh} in oocytes injected with membranes from the two groups of patients (Table S1), selecting the membrane preparations that produced the largest ACh-evoked responses. We first analyzed AChR desensitization in oocytes injected with muscle membranes obtained from ALS or denervated patients. During prolonged applications of ACh (250 μM for 2 min), I_{ACh} showed a decay (Fig. 1*C*) that was adequately fitted by a single exponential function. The decay time constants were similar in oocytes injected with membranes from ALS (τ_{decay} = 9.8± 0.7 s, 15/3; P1 and P5) or denervated patients (τ_{decay} = 8.9 ± 0.3 s, 15/3; P20 and P21; $P > 0.05$). We also measured current decays during repetitive ACh applications (100 μM, 5-s duration, 40-s interval). In oocytes injected with ALS muscle membranes (P1, P4, P9, and P10) the peak amplitude of the 10th I_{ACh} was 53 ± 6% (10/3) of the first, comparable to that observed in oocytes injected with denervated muscle membranes (55 ± 5%, 10/3 frogs; P20, P21, and P25,), showing that AChR desensitization is similar in muscles of ALS or denervated patients under the experimental conditions used here.

The ACh dose–current response relation in oocytes injected with membranes from five denervated patients (P20–22, P24, and P25; Fig. 2*A*) yielded half-maximal effect (EC_{50}) and n_H values of 33 ± 3 μM and 1.4 ± 0.1, respectively (28/3). In oocytes injected with membranes isolated from ALS muscles (P1, P4–6, P8; Fig. 2*A*) the EC_{50} was significantly greater (56 ± 3 μM, 28/3; $P < 0.05$), whereas n_H was unchanged (1.4 ± 0.1). The current–voltage relation showed slight inward rectification for both groups of patients (Fig. 2*B*) and the reversal potential for I_{ACh} was similar in oocytes injected with ALS (−5.1 ± 0.2 mV; 10/3 ; P1, P5, and P9) or denervated muscle membranes (−4.4 ± 0.2 mV, 8/3; P20 and P21).

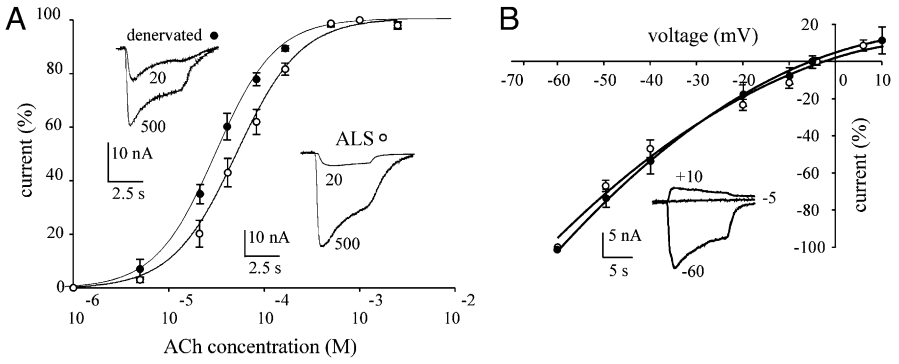

Fig. 2. Characterization of ACh-evoked currents in injected oocytes. (*A*) Amplitude of currents evoked by various ACh concentrations, expressed as percentage of the maximal current evoked by 1 mM ACh, plotted as mean ± SEM and best fitted with Hill curves. Averaged EC_{50} values and n_H in oocytes injected with membranes from denervated patients were 33 ± 3 μM and 1.4 ± 0.1 (●; 28 oocytes/3 frogs; five patients); for ALS patients values were 56 ± 2.6 μM and 1.4 ± 0.1 (○; 28/3; five patients). (*Inset*) Currents elicited by the indicated ACh concentrations (in μM) in oocytes injected with ALS (*Right*) or denervated membranes (*Left*) as indicated. (*B*) ACh current–voltage relation in oocytes injected with denervated (●, 8/3; two patients) or ALS muscle membranes (○, 10/3; three patients). In each cell, the peak amplitudes of ACh-evoked (100 μM) currents were normalized to that evoked at −60 mV. Reversal potentials of I_{ACh} were −4.4 ± 0.2 mV (●) and −5.1 ± 0.2 mV (○). (*Inset*) Sample traces of I_{ACh} elicited at the holding potentials indicated (mV) in 1 oocyte injected with ALS membranes.

Functional Effects of Drugs Used in ALS Therapy on Human Muscle AChRs. Riluzole blocks mouse nicotinic AChR in transfected HEK-293 cells (17) and membrane-injected oocytes represent an ideal preparation for testing the effect of riluzole on AChRs derived from muscles of ALS patients (Fig. 3). In 12 oocytes injected with membranes from ALS patients (P1 and P5), currents evoked by ACh (100 μM) were blocked by riluzole (coapplied with ACh after a 20-s pretreatment) with half-inhibitory concentration (IC_{50}) of 22.3 ± 5 μM and n_H = 1.0 ± 0.2. Similar values of IC_{50} and n_H (23.8 ± 5 μM and 1.0 ± 0.1; 12/2) were obtained in oocytes injected with membranes from denervated patients (P20 and P21; Fig. 3).

Because riluzole plasma concentration in ALS patients is in a range of 0.5 to 5 μM (2), we performed additional experiments using riluzole at a clinically relevant concentration (0.5 μM), increasing the duration of pretreatment to 2 min. With this application protocol, riluzole caused the I_{ACh} to decrease to 71 ± 7% (8/2) and 72 ± 9% (8/2) in oocytes injected with muscle membranes from ALS (P1 and P5) and denervated patients (P20 and P21), respectively. The block was completely reversible after 4 min of washout.

To exploit further the potential of our experimental preparation, we studied the effects of galantamine and erythropoietin (Epo), two drugs that have been proposed as therapeutics for ALS and that could affect the function of muscle AChR. Galantamine is an acetylcholinesterase inhibitor used for Alzheimer's disease; at low concentrations it can weakly activate muscle AChRs, whereas it acts as an open channel blocker at higher concentrations (21, 22). In oocytes injected with ALS membranes (P1 and P9; 9/2 oocytes) galantamine failed to evoke currents but blocked currents evoked by ACh (250 μM) in a dose-dependent manner (10–500 μM, 30-s pretreatment; 20/3; Fig. 4*A*). As for many open-channel blockers, galantamine-induced block of I_{ACh} was fully reversible and voltage dependent. For example, application of 500 μM galantamine reduced I_{ACh} amplitude to 16 ± 2% of control at −100 mV and to 79 ± 4% at −20 mV (8/2; $P < 0.05$). In contrast to galantamine, Epo (5–10 units/mL), which has recently been suggested as a new drug for ALS because of its neuroprotective properties (23), had no significant effect on the I_{ACh} amplitude or decay in these oocytes (15/3; e.g., Fig. 4*B*; P1 and P9).

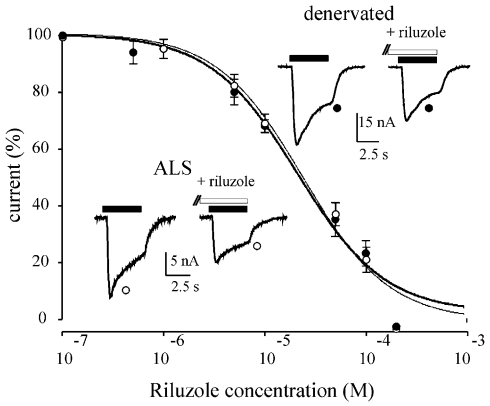

Fig. 3. Inhibition of ACh-evoked currents by riluzole in oocytes injected with muscle membranes from denervated (●, 12 oocytes/2 frogs; two patients) or ALS patients (○, 12/2; two patients). The amplitudes of currents evoked by ACh (100 μM, −60 mV) plus riluzole are expressed as percentage of control currents (ACh alone). IC_{50} and n_H were 23.8 ± 5 μM and 1.0 ± 0.1 (●); 22.3 ± 5 μM and 1.0 ± 0.2 (○). The sample traces represent currents elicited by ACh (100 μM) alone or in the presence of riluzole (20μM, open bar) in two oocytes, injected with ALS or denervated membranes, as indicated.

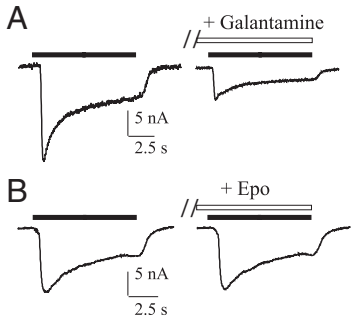

Fig. 4. (*A*) Sample current traces elicited by 250 μM ACh before and after treatment with 500 μM galantamine (open bar) in 1 oocyte (representative of 20) injected with ALS muscle membranes (P9, Table S1). (*B*) Current traces elicited by 100 μM ACh before and after treatment with 10 units/mL Epo (open bar) in 1 oocyte (representative of 15) injected with ALS muscle membranes (P9, Table S1).

Patch-Clamp Recordings on Myotubes from ALS Patients. We derived polynucleated myotubes from ALS and denervated muscles and studied their AChR channels using patch-clamp recordings. Cultures derived from either denervated or ALS patients contained comparable percentages of myogenic, desmin$^+$ cells (14 ± 3%, n = 4 vs. 14 ± 2%, n = 8) and yielded myotubes of equivalent size, as revealed by similar fusion index (62 ± 1%, n = 4 vs. 43 ± 1%, n = 8; $P > 0.05$) and membrane capacitance (80.2 ± 5.9 pF, n = 30 vs. 78.1 ± 6.5 pF, n = 41; $P > 0.05$). ACh concentration–current response curves were similar in the two sets of cells, as was the density of ACh-evoked whole cell currents (Fig. 5 *A* and *B*). At a concentration of 100 μM, ACh evoked currents decayed exponentially, with time constants (τ_{decay}) of 156 ± 11 ms (n = 30) or 150 ± 10 ms (n = 41) for myotubes obtained from denervated and ALS patients, respectively (Fig. 5*A*). Riluzole reduced the amplitude and accelerated the decay of ACh-evoked currents in all myotubes tested. When a clinically relevant concentration of riluzole (0.5 μM) was applied 30 s before coapplication with ACh (100 μM), current amplitude was decreased to 67 ± 4% (n = 13) and τ_{decay} to 63 ± 3% of the control values measured in the same myotubes from denervated patients. In ALS myotubes, amplitude and τ_{decay} were reduced to 60 ± 4% and 69 ± 2% (n = 15), respectively (Fig. 5*A*).

When cells were bathed in normal extracellular saline (NES), ACh-evoked unitary events were recorded in 60% of patched myotubes obtained from denervated patients but only in 20% of the ALS myotubes (Fig. 5*C*), largely because seals were unstable in the latter preparation. Most experiments were therefore performed on myotubes bathed in a KCl-based extracellular solution, with NES plus ACh (0.1 μM) in the patch pipette. Channel slope conductance was 35.3 ± 1.8 pS (n = 9) in myotubes from denervated patients and 36.9 ± 1.3 pS (n = 10) for ALS myotubes. In all cases, the distribution of channel open duration was adequately fitted by two exponential components with similar time constants (e.g., Fig. 5*C*). Channel closed duration showed large patch-to-patch variations, likely reflecting the number of channels within each patch.

Discussion

In this paper we present proof of principle that muscle specimens donated by ALS or denervated patients through minimally invasive procedures can be used for microtransplantation of AChRs by membrane injection into *Xenopus* oocytes (18, 19) and for generating polynucleated myotubes from muscle satellite cells. Both experimental preparations allow detailed functional studies of AChR channels and other muscle ion channels. These methods will be valuable in testing the currently emerging hypothesis that the neuromuscular junction represents the site of disease onset

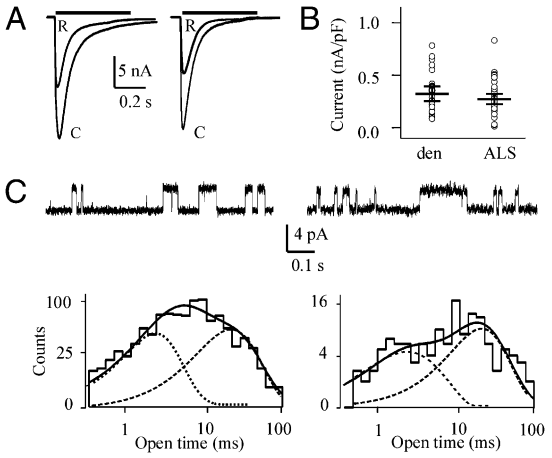

Fig. 5. ACh-evoked currents in myotubes. (*A*) Typical whole-cell current responses evoked by ACh (100 μM; −60 mV) alone (*C*) or together with riluzole (R; 0.5 μM, 30-s pretreatment) in myotubes derived from a denervated patient (*Left*, P28) and an ALS patient (*Right*, P19). (*B*) Dispersion plot of control ACh-evoked current density in all myotubes tested. Bars represent mean ± 95% confidence interval of values. (*C*) ACh-evoked unitary channel openings (upward) in myotubes from a denervated patient (P27, *Left*) and an ALS patient (P18, *Right*). Channel conductances were 33.5 pS (*Left*) and 30 pS (*Right*). The distribution of channel open duration in these recordings was best fitted with the sum (continuous lines) of two exponential components (dotted lines), with time constants 3.2 ms (44%) and 16.6 ms (56%) (*Left*); 1.6 ms (38%) and 16.2 ms (62%) (*Right*).

and that skeletal muscle directly contributes to ALS pathogenesis (1, 4, 5), the so-called "dying-back model."

Microtransplantation of muscle-type AChR has been achieved before (24, 25); here we demonstrate the feasibility of this procedure when starting from tiny muscle samples, indicating that this approach is efficacious for studies of AChRs in human muscle diseases. Cultured myotubes from needle biopsies have also been obtained by others (26), but to our knowledge this is a unique study performing functional studies on myotubes derived from patients with a disease reported to reduce the differentiative capacity of the satellite cells (20).

The action of nicotine, the current–voltage relationship, and the effects of classical nicotinic antagonists indicate that the ACh-evoked currents measured in muscle membrane-injected oocytes are due to the activation of bona fide nicotinic AChRs derived from the patients' muscles. A modest rectification in current–voltage relation for human muscle γ-AChR channels has been previously observed in native preparations (27, 28).

No difference was found when comparing the functional properties of AChRs in myotubes derived from the two groups of patients, matching previous reports for human myotubes derived from healthy subjects (28) and for reconstituted γ-AChR channels (16). These data suggest that satellite cells from ALS patients, when exposed to the standardized culture medium, yield myotubes expressing "normal" γ-AChR, as expected from their developmental program. ACh-evoked currents of oocytes injected with muscle membranes from ALS or denervated patients showed an almost identical pattern of AChR desensitization, indicating that this receptor property is not altered in ALS patients. Conversely, there was a small but significant difference in ACh sensitivity. The larger EC_{50} observed for ALS AChRs in injected oocytes could be due to a variable proportion of γ- and ε-AChRs in the muscle membranes derived from ALS patients, reflecting the cycles of denervation/reinnervation typical of ALS. Values reported for human γ- or ε-AChR (29, 30) are in the same range, as the EC_{50} we report for AChR from denervated patients. Whereas it is clear that human myotubes from ALS or denervated patients express the fetal form of the AChR, our biopsied muscle tissues from ALS patients transplanted in oocytes may express mixed γ/ε-containing receptors. Further experiments using quantitative RT-PCR or immunostaining procedures will provide tests of this hypothesis. However, because the microtransplantation procedure leads to incorporation into the oocyte membrane of receptors still embedded in their native membrane, other factors may affect the EC_{50} for ACh in this preparation. Membrane lipids modulate ACh-evoked responses in dystrophic mouse myotubes (31) and induce loss of function of AChR reconstituted in mammalian cells (32). Differences in membrane lipid composition could also account for the reduced stability of cell-attached patches experienced when recording from myotubes derived from ALS patients.

It has been reported recently that riluzole can induce a delay in the progression of the disease and reduce extensive use of artificial ventilation in ALS patients (2). Riluzole blocks voltage-gated sodium channels plus a variety of other channels (33–35) and inhibits ACh currents in transfected cell lines at very high concentrations (17). However, to date there have been no studies of AChRs in ALS muscles (2). In this study we used two different technical approaches, both of which showed that riluzole, at clinically relevant doses, can block the ACh-evoked currents in ALS patients as well as in denervated patients. Because ongoing myogenesis has been reported in muscle biopsies of ALS or traumatically denervated patients (36), innervation of newly formed muscle fibers likely proceeds alongside reinnervation of old fibers by surviving motor neurons in ALS patients. The activity of AChRs plays a role in both processes. Whether or not riluzole interferes with this process becomes an interesting open question. We also tested two other drugs, galantamine and Epo, which have been recently suggested as alternative therapeutic drugs for ALS (21, 23). Our voltage-dependent block of I_{ACh} by galantamine is in good agreement with previous findings on AChRs reconstituted in HEK cells (22), whereas Epo does not affect these currents. Responses induced by low concentrations of galantamine likely remained below detection threshold due to the low potency of this agonist in our system. The reported therapeutic action of these drugs may not be related to their effect on postsynaptic muscle AChRs but to their action on presynaptic mechanisms such as glutamate release or neuronal cholinergic activation (21, 37) that we cannot explore with our preparations. In conclusion, the present work helps to understand the mechanisms underlying ALS pathology by (*i*) providing simple but powerful techniques to study the muscle physiopathology of ALS using small amounts of tissue obtained through muscle biopsies; and (*ii*) suggesting that muscle AChRs could be a target for new drugs paving the way for developing alternative strategies toward the medical treatment of ALS (38).

Materials and Methods

Patients. We obtained muscle specimens from 19 ALS patients (P1–19, Table S1) and 9 control patients with muscle denervation due to other causes (P20–28, Table S1). All patients were recruited and examined by the neurologists (directed by M.I.) at the Neuromuscular Disease Unit of the Policlinico Umberto I, Sapienza University, Rome. *SI Materials and Methods* provides further details. Informed consent to use part of the biopsy material for our experiments was obtained from all patients. The human subjects ethical committee of Sapienza University approved the selection process and surgical procedures.

Membrane Preparation, Injection Procedures, and Electrophysiological Recordings from Oocytes. Human muscle specimens (10–100 mg) were frozen in liquid nitrogen immediately after biopsy and stored at −80 °C. Membranes were prepared as previously detailed (39). Preparation of *Xenopus laevis* oocytes and injection procedures were as detailed elsewhere (39, 40). Membrane currents were recorded from voltage-clamped oocytes 24–48 h after injection using two microelectrodes filled with 3 M KCl. The oocytes were placed in a recording chamber (volume, 0.1 mL) and perfused

continuously, 9–10 mL/min, with oocyte Ringer's solution (OR) at room temperature (20–22 °C). Unless otherwise specified, the oocytes were voltage clamped at −60 mV. To construct current–voltage (*I–V*) relationships, the membrane potential was stepped to the desired values 2–4 min before applying ACh. To determine the reversal of I_{ACh}, *I–V* relationships were fitted with a second order polynomial using pClamp 10 software. Decreases in I_{ACh} during repetitive ACh applications (100 μM for 5 s at 40-s intervals) were quantified by expressing the peak amplitude of the 10th response as a percentage of the peak amplitude of the first. Rapid I_{ACh} desensitization was measured by fitting ACh currents with a first order exponential function and calculating the time constant (τ_{decay}).

The IC_{50} of riluzole and the ACh concentration producing EC_{50} were estimated by fitting the data to Hill equations, using least-square routines as previously described (40).

Galantamine hydrobromide (Tocris), riluzole hydrochloride (Sigma or Tocris), human Epo, α-bungarotoxin, d-tubocurarine, ACh, and nicotine were dissolved in OR just before use. Where not indicated, drugs were purchased from Sigma. Data were analyzed using Sigma Plot software and are given as means ± SEM; datasets are considered statistically different when $P < 0.05$. (ANOVA test). *SI Materials and Methods* provides further information.

Cell Culture and Patch-Clamp Recordings in Myotubes. Human myotubes were obtained from satellite cells derived from human muscle needle biopsies obtained as above, using previously reported procedures for culture (16) and staining (41), as detailed in *SI Materials and Methods*. Cultures were maintained in a humidified incubator with 5% CO_2, at 37 °C. All of the media were purchased from Gibco/Invitrogen, except for the epidermal growth factor (Sigma). Patch-clamp recordings were performed using borosilicate glass patch pipettes (3–5 MΩ tip resistance, Sylgard coated for single-channel recordings) connected to an Axopatch 200B amplifier (Molecular Devices) driven by pCLAMP9 software (Molecular Devices). In whole-cell experiments, cell capacitance and patch series resistance (5–15 MΩ) were estimated from slow transient compensations, with a series resistance compensation of 80–95%. Cells were voltage clamped at a holding potential (HP) of -60 mV (unless otherwise indicated) and continuously superfused using a gravity-driven perfusion system with independent tubes for standard and agonist-containing solutions positioned 50–100 μm from the patched cell using a fast exchanger system (RSC-200; BioLogique). Normal extracellular solution (NES) contained (mM): NaCl 140, KCl 2.8, $CaCl_2$ 2, $MgCl_2$ 2, Glucose 10, Hepes/NaOH 10, pH 7.3; intracellular solution contained (mM), CsCl 140, $MgCl_2$ 2, BAPTA 5, Hepes/CsOH 10, Mg-ATP 2, pH 7.3. For cell-attached recordings, an extracellular solution with swapped concentrations of NaCl and KCl was used.

Single-channel data were recorded sampling at 25 kHz. Cells were bathed in a solution containing (mM): KCl 140, Na 2.8, $CaCl_2$ 2, $MgCl_2$ 2, Glucose 10, Hepes/NaOH 10, pH 7.3, whereas pipettes were filled with NES. Analysis was performed after Gaussian filtering at 2.5 kHz with a 50% threshold criterion using pClamp9 software.

Data are given as means ± SEM. Two datasets were considered statistically different when $P < 0.05$ (ANOVA test).

ACKNOWLEDGMENTS. We thank Drs. Nick Spitzer and Enzo Wanke for critical reading of the manuscript and we are extremely grateful to all the patients whose generous donation of tissues made this study possible. This work was supported by grants from the Association Against ALS, Fondazione Viva La Vita (to M.I. and C.L.); Ministero della Salute Antidoping project (to C.L and E.P.), the French Association against Myopathies, (to F.G.); and Ministero dell'Istruzione, dell'Università e della Ricerca (to E.P. and C.L.). L.C. and C.D. were supported by the Neurophysiology PhD program, University of Sapienza.

1. Musarò A (2010) State of the art and the dark side of amyotrophic lateral sclerosis. *World J Biol Chem* 1:62–68.
2. Bellingham MC (2011) A review of the neural mechanisms of action and clinical efficiency of riluzole in treating amyotrophic lateral sclerosis: What have we learned in the last decade? *CNS Neurosci Ther* 17:4–31.
3. Frey D, et al. (2000) Early and selective loss of neuromuscular synapse subtypes with low sprouting competence in motoneuron diseases. *J Neurosci* 20:2534–2542.
4. Dadon-Nachum M, Melamed E, Offen D (2011) The "dying-back" phenomenon of motor neurons in ALS. *J Mol Neurosci* 43:470–477.
5. Dupuis L, Loeffler JP (2009) Neuromuscular junction destruction during amyotrophic lateral sclerosis: Insights from transgenic models. *Curr Opin Pharmacol* 9:341–346.
6. Dobrowolny G, et al. (2005) Muscle expression of a local Igf-1 isoform protects motor neurons in an ALS mouse model. *J Cell Biol* 168:193–199.
7. Nakanishi ST, Cope TC, Rich MM, Carrasco DI, Pinter MJ (2005) Regulation of motoneuron excitability via motor endplate acetylcholine receptor activation. *J Neurosci* 25:2226–2232.
8. Fischer LR, et al. (2004) Amyotrophic lateral sclerosis is a distal axonopathy: Evidence in mice and man. *Exp Neurol* 185:232–240.
9. Miledi R (1960) Junctional and extra-junctional acetylcholine receptors in skeletal muscle fibres. *J Physiol* 151:24–30.
10. Miledi R, Trowell OA (1962) Acetylcholine sensitivity of rat diaphragm maintained in organ culture. *Nature* 194:981–982.
11. Katz B, Miledi R (1964) Further observations on the the distribution of acetylcholine: Reactive sites in skeletal muscle. *J Physiol* 170:379–388.
12. Miledi R (1960) The acetylcholine sensitivity of frog muscle fibres after complete or partial deervation. *J Physiol* 151:1–23.
13. Cull-Candy SG, Miledi R, Uchitel OD (1982) Denervation changes in normal and myasthenia gravis human muscle fibres during organ culture. *J Physiol* 333:227–249.
14. Witzemann V, Brenner HR, Sakmann B (1991) Neural factors regulate AChR subunit mRNAs at rat neuromuscular synapses. *J Cell Biol* 114:125–141.
15. Villarroel A, Sakmann B (1996) Calcium permeability increase of endplate channels in rat muscle during postnatal development. *J Physiol* 496:331–338.
16. Fucile S, Sucapane A, Grassi F, Eusebi F, Engel AG (2006) The human adult subtype ACh receptor channel has high Ca^{2+} permeability and predisposes to endplate Ca^{2+} overloading. *J Physiol* 573:35–43.
17. Mohammadi B, Lang N, Dengler R, Bufler J (2002) Interaction of high concentrations of riluzole with recombinant skeletal muscle sodium channels and adult-type nicotinic receptor channels. *Muscle Nerve* 26:539–545.
18. Miledi R, Eusebi F, Martínez-Torres A, Palma E, Trettel F (2002) Expression of functional neurotransmitter receptors in Xenopus oocytes after injection of human brain membranes. *Proc Natl Acad Sci USA* 99:13238–13242.
19. Eusebi F, Palma E, Amici M, Miledi R (2009) Microtransplantation of ligand-gated receptor-channels from fresh or frozen nervous tissue into Xenopus oocytes: A potent tool for expanding functional information. *Prog Neurobiol* 88:32–40.
20. Pradat PF, et al. (2011) Abnormalities of satellite cells function in amyotrophic lateral sclerosis. *Amyotroph Lateral Scler* 12:264–271.
21. Nakamizo T, et al. (2005) Stimulation of nicotinic acetylcholine receptors protects motor neurons. *Biochem Biophys Res Commun* 330:1285–1289.
22. Akk G, Steinbach JH (2005) Galantamine activates muscle-type nicotinic acetylcholine receptors without binding to the acetylcholine-binding site. *J Neurosci* 25:1992–2001.
23. Butsch PO, Cudkowicz ME (2007) Is erythropoietin a potential therapy for amyotrophic lateral sclerosis? *Exp Neurol* 206:11–15.
24. Marsal J, Tigyi G, Miledi R (1995) Incorporation of acetylcholine receptors and Cl-channels in Xenopus oocytes injected with Torpedo electroplaque membranes. *Proc Natl Acad Sci USA* 92:5224–5228.
25. Bernareggi A, Reyes-Ruiz JM, Lorenzon P, Ruzzier F, Miledi R (2011) Microtransplantation of acetylcholine receptors from normal or denervated rat skeletal muscles to frog oocytes. *J Physiol* 589:1133–1142.
26. Magistris MR, et al. (1998) Needle muscle biopsy in the investigation of neuromuscular disorders. *Muscle Nerve* 21:194–200.
27. Grassi F, Giovannelli A, Fucile S, Mattei E, Eusebi F (1993) Cholinergic responses in cloned human TE671/RD tumour cells. *Pflugers Arch* 425:117–125.
28. Krause RM, et al. (1995) Activation of nicotinic acetylcholine receptors increases the rate of fusion of cultured human myoblasts. *J Physiol* 489:779–790.
29. Shao Z, Mellor IR, Brierley MJ, Harris J, Usherwood PN (1998) Potentiation and inhibition of nicotinic acetylcholine receptors by spermine in the TE671 human muscle cell line. *J Pharmacol Exp Ther* 286:1269–1276.
30. Moriconi C, Di Castro MA, Fucile S, Eusebi F, Grassi F (2010) Mechanism of verapamil action on wild-type and slow-channel mutant human muscle acetylcholine receptor. *J Neurochem* 114:1231–1240.
31. Eusebi F, Cossu G, Molinaro M, Giacomoni D (1986) Liposome-delivered phosphatidylcholine enhances the acetylcholine sensitivity of dystrophic mouse myotubes. *Biochim Biophys Acta* 855:197–199.
32. Borroni V, et al. (2007) Cholesterol depletion activates rapid internalization of submicron-sized acetylcholine receptor domains at the cell membrane. *Mol Membr Biol* 24:1–15.
33. Yvon C, Czarnecki A, Streit J (2007) Riluzole-induced oscillations in spinal networks. *J Neurophysiol* 97:3607–3620.
34. Lamanauskas N, Nistri A (2008) Riluzole blocks persistent Na^+ and Ca^{2+} currents and modulates release of glutamate via presynaptic NMDA receptors on neonatal rat hypoglossal motoneurons in vitro. *Eur J Neurosci* 27:2501–2514.
35. Gullo F, et al. (2010) Orchestration of "presto" and "largo" synchrony in up-down activity of cortical networks. *Front Neural Circuits* 4:11.
36. Doppler K, Mittelbronn M, Bornemann A (2008) Myogenesis in human denervated muscle biopsies. *Muscle Nerve* 37:79–83.
37. Nagańska E, Taraszewska A, Matyja E, Grieb P, Rafałowska J (2010) Neuroprotective effect of erythropoietin in amyotrophic lateral sclerosis (ALS) model in vitro. Ultrastructural study. *Folia Neuropathol* 48:35–44.
38. Zinman L, Cudkowicz M (2011) Emerging targets and treatments in amyotrophic lateral sclerosis. *Lancet Neurol* 10:481–490.
39. Miledi R, Palma E, Eusebi F (2006) Microtransplantation of neurotransmitter receptors from cells to Xenopus oocyte membranes: New procedure for ion channel studies. *Methods Mol Biol* 322:347–355.
40. Palma E, et al. (2002) Expression of human epileptic temporal lobe neurotransmitter receptors in Xenopus oocytes: An innovative approach to study epilepsy. *Proc Natl Acad Sci USA* 99:15078–15083.
41. Grassi F, et al. (2004) Fusion-independent expression of functional ACh receptors in mouse mesoangioblast stem cells contacting muscle cells. *J Physiol* 560:479–489.

Supporting Information

Palma et al. 10.1073/pnas.1117975108

SI Materials and Methods

Patients. ALS patients (8 females, 11 males, mean age 64.5 ± 9.2 y, Table S1) were recruited from the ALS Center of Policlinico Umberto I, Università Sapienza of Rome, directed by M.I. All 19 patients had probable or definite ALS (1); 17 patients had a spinal onset disease, whereas the other 2 had a bulbar and pseudobulbar onset disease. Mean time from diagnosis at the time of muscle biopsy was 23.5 ± 14.4 mo. Patients were clinically assessed with the ALS Functional Rating Scale-Revised (2). The scale ranges from 48 points (in a healthy individual) to 0 (patient in locked-in condition, with respiratory assistance and artificial nutrition); mean score at the time of muscle biopsy was 26 ± 11.

Control denervated patients (three females, six males, mean age 47.2 ± 14.6 y, Table S1) had neurogenic lesions due to trauma or peripheral neuropathies; mean duration of disease was widely variable ranging from 2 wk to 10 y. Both ALS and control denervated patients underwent needle electromyography of several muscles before muscle biopsy to assess denervation grade; the muscle in which biopsy was performed, was decided accordingly. Five muscle sites were sampled and 1 point was assigned for each insertion site where denervation potentials could be observed (max = 5). Thus, biopsy samples were characterized according to the degree of denervation consistently among patients, as reported in Table S1.

Membrane Preparation. Briefly, tissues were homogenized using a Teflon glass homogenizer with 2 mL of glycine buffer of the following composition (in mM): 200 glycine, 150 NaCl, 50 EGTA, 50 EDTA, 300 sucrose; plus 20 μL protease inhibitors (cat. no. P2714; Sigma); pH 9 adjusted with NaOH. The homogenate was centrifuged for 15 min at 9,500 × *g* in a Beckmann centrifuge (C1015 rotor). The supernatant was collected and centrifuged for 2 h at 10^5 × *g* in a TL-100 rotor at 4 °C. The pellet was washed, resuspended in assay buffer (glycine 5 mM), and used directly or stored at −80 °C for later use.

Myotube Preparation and Characterization. Muscle fragments were mechanically dissociated after digestion with collagenase and dispase (3.5 mg/mL and 2 units/mL for 50 min at 37 °C). Cells were allowed to proliferate on collagen-coated Petri dishes in DMEM supplemented with 15% FCS, 2% penicillin/streptomycin (P/S), 1% insulin-transferrin-selenium, and 10 ng/mL epidermal growth factor. Differentiation was induced at ∼50% confluence by switching to a low-serum medium (DMEM plus 2% horse serum and P/S). Fusion index, defined as the ratio of the number of nuclei in multinucleated cells to the total number of nuclei in desmin$^+$ cells in the field, was measured, counting 38 fields of four preparations (400× magnification) and 80 fields of eight preparations for myotubes from denervated and ALS patients, respectively. Immunofluorescence analysis was carried out using a mouse antidesmin monoclonal antibody (clone D33, Dako). Briefly, cell cultures were washed with PBS (Gibco), fixed with paraformaldehyde 4% for 15 min, and permeabilized with 0.1% Triton X-100 for 3 min. Cells were kept for 60 min at room temperature with blocking solution (PBS containing 1% BSA), then incubated with primary antibody overnight at 4 °C. At the end of incubation, the cells were washed with PBS and incubated for 1 h at room temperature with Alexa Fluor 488 donkey antimouse IgG (1:2,000 dilution; Invitrogen). Nuclei were stained with Hoechst 33342 trihydrochloride, trihydrate (Invitrogen). Cultures were observed under a Zeiss Axiophot epifluorescence microscope.

1. Brooks BR (1994) El Escorial World Federation of Neurology criteria for the diagnosis of amyotrophic lateral sclerosis. Subcommittee on Motor Neuron Diseases/Amyotrophic Lateral Sclerosis of the World Federation of Neurology Research Group on Neuromuscular Diseases and the El Escorial "Clinical limits of amyotrophic lateral sclerosis" workshop contributors. *J Neurol Sci* 124(Suppl):96–107.

2. Cedarbaum JM, et al.; BDNF ALS Study Group (Phase III) (1999) The ALSFRS-R: A revised ALS functional rating scale that incorporates assessments of respiratory function. *J Neurol Sci* 169:13–21.

Table S1. Clinical characteristics of ALS and denervated control patients

Patient (P)	Sex	Age, y	Pathology (phenotype)	Disease duration	ALSFRS-R score	Site of biopsy	Denervation grade
1	F	58	ALS (spinal)	14 mo	22	Deltoid	1
2	F	59	ALS (bulbar)	15 mo	10	Deltoid	1
3	F	54	ALS (spinal)	16 mo	42	Deltoid	1
4	M	55	ALS (spinal)	26 mo	24	Deltoid	4
5	M	63	ALS (spinal)	12 mo	23	Deltoid	4
6	M	70	ALS (spinal)	32 mo	19	Deltoid	4
7	M	70	ALS (spinal)	7 mo	35	Deltoid	2
8	M	73	ALS (spinal)	4 mo	33	Quadriceps	2
9	F	57	ALS (spinal)	33 mo	17	Deltoid	2
10	M	61	ALS (pseudobulbar)	15 mo	42	Deltoid	2
11	F	77	ALS (spinal)	19 mo	16	Deltoid	2
12	M	70	ALS (spinal)	60 mo	31	Deltoid	2
13	F	79	ALS (spinal)	36 mo	20	Deltoid	4
14	M	44	ALS (spinal)	36 mo	13	Deltoid	4
15*	F	73	ALS (spinal)	36 mo	5	Anterior tibialis	3
16*	F	62	ALS (spinal)	8 mo	36	Anterior tibialis	4
17*	M	75	ALS (spinal)	42 mo	30	Anterior tibialis	3
18*	M	59	ALS (spinal)	24 mo	48	Deltoid	2
19*	M	67	ALS (spinal)	12 mo	35	Anterior tibialis	5
20	M	40	Polytrauma	3 wk	—	Anterior tibialis	4
21	M	35	Polytrauma	3 wk	—	Quadriceps	4
22	M	65	Polytrauma	2 mo	—	Anterior tibialis	4
23	M	70	CIDP	10 y	—	Anterior tibialis	2
24	M	30	Peroneal nerve lesion	1 mo	—	Anterior tibialis	4
25	F	42	Axonal neuropathy	36 mo	—	Anterior tibialis	4
26*	F	40	Polytrauma	3 wk	—	Anterior tibialis	5
27*	F	63	Sciatic nerve lesion	24 mo	—	Anterior tibialis	4
28*	M	40	Polytrauma	2 wk	—	Anterior tibialis	4

ALS, amyotrophic lateral sclerosis; ALSFRS-R, Amyotrophic Lateral Sclerosis Functional Rating Scale-Revised, 1–48; denervation grade, 1–5; CIDP, chronic inflammatory demyelinating polyneuropathy (*SI Materials and Methods* for refs. 1 and 2). All biopsies were used to measure mean ACh current; some were selected to test drugs or functional properties.
*Patch-clamp recordings on cultured myotubes.